


Rapid Protein–Ligand Costructures from Sparse NOE Data

Dipen M. Shah,^{†,‡} Eiso AB,[‡] Tammo Diercks,[§] Mathias A. S. Hass,[†] Nico A. J. van Nuland,^{||} and Gregg Siegal^{*,†,‡}[†]Leiden Institute of Chemistry, Leiden University, Leiden 2300RA, The Netherlands[‡]ZoBio BV, Leiden 2300RA, The Netherlands[§]Centre for Co-operative Research in Biosciences, Derio 48160, Spain^{||}Jean Jeener NMR Centre, Structural Biology, Vrije Universiteit Brussel and Molecular Recognition Unit, VIB Department of Structural Biology, Brussels 1050, Belgium Supporting Information

ABSTRACT: An efficient way to rapidly generate protein–ligand costructures based on solution-NMR using sparse NOE data combined with selective isotope labeling is presented. A docked model of the 27 kDa N-terminal ATPase domain of Hsp90 bound to a small molecule ligand was generated using only 21 intermolecular NOEs, which uniquely defined both the binding site and the orientation of the ligand. The approach can prove valuable for the early stages of fragment-based drug discovery.

 INTRODUCTION

The availability of 3D structural information on protein–ligand complexes has become an important driver to guide the preclinical stages of drug discovery. Structure-based drug design (SBDD) has enabled the development of a wide array of drugs that are currently on the market such as inhibitors of the HIV protease and kinases.^{1,2} In the past 15 years, fragment-based drug discovery (FBDD), which uses very small, soluble drug fragments as starting points to develop new medicines, has become widespread. Because of their small size, fragments typically bind the target with low affinity ($K_D > 10 \mu\text{M}$). The development of weak fragment hits to more potent lead-like structures is 2–3 times more successful when 3D structural information is available.³ Thus the success of both SBDD and FBDD is heavily dependent upon the availability of structural information. Presently, both approaches are primarily driven by X-ray crystallography. Crystallography has the advantage that when successful, it is both rapid and high resolution. However, there are a number of cases in which crystallography is not successful such as when crystals are not available, the crystal packing precludes access to the active site or most commonly, weakly binding fragments simply do not give rise to electron density. In the latter case, there can be many causes including insufficient occupancy of the binding site or multiple possible binding orientations. In principle, NMR-based solution methods can also generate atomic resolution structural information and NMR has indeed successfully supported FBDD campaigns.⁴ Because NMR is extremely sensitive to weak protein–ligand interactions, it should be applicable exactly where crystallography is least effective, i.e., for complexes of weakly binding ligands. However, traditional NMR approaches involving uniform isotopic labeling are labor intensive and limited to proteins of moderate size (e.g., < 30 kDa) and have therefore not been widely adopted in drug discovery.

In drug discovery it is often the case that the 3D structure of a target or a homologous protein is available. If the resonance

assignment of such a protein is available, mapping of chemical shift perturbations (CSPs) onto the 3D structure is a simple, fast procedure that can provide low-resolution information about a small-molecule binding site.⁵ CSP mapping is most commonly accomplished through analysis of ¹⁵N- or ¹³C-edited heteronuclear correlation spectra of the protein. However, the interpretation of ¹H–¹⁵N or ¹H–¹³C HSQC CSPs becomes ambiguous when the chemical shift perturbations are caused by changes in protein dynamics or a shift in equilibrium between two (or more) conformations. Various computational methods based on primarily chemical shift perturbation analysis are most successful at determining the location of the binding site to low resolution. The precise nature of the intermolecular contacts are well beyond the capabilities of structural analysis based on CSPs.^{6,7} In principle, a limited set of intermolecular NOEs could provide sufficient information to determine the orientation and binding mode of a small molecule bound to a protein. Indeed, a number of approaches that use a combination of amino acid selective labeling and intermolecular NOEs have been proposed.^{8–10} While these are quite powerful, they suffer from one or more of the following limitations: (i) requirement for a priori knowledge of the ligand binding site in order to be able to efficiently select the right combination of residues to label, (ii) requirement for a large number of intermolecular NOE contacts, (iii) the resonance assignment uses the pattern of chemical shift perturbations induced by ligand binding and therefore may not be robust, and (iv) requirement for extensive calculations to generate structures that match the experimental data. We sought an NMR-based method capable of providing structures of sufficient resolution and reliability to support elaboration of “weakly” binding fragments to target proteins that met the following criteria: widely applicable to small and large proteins, rapid (2–3 weeks per complex), standard solution conditions and NMR experi-

Received: September 27, 2012

Published: November 12, 2012

ments, requires samples that can be easily made, and the data interpretation is unambiguous. Here, we demonstrate such a method based on selective ILV methyl-labeling and a sparse set of intermolecular NOEs.

RESULTS AND DISCUSSION

The approach as outlined in Supporting Information (SI) Figure S1, requires an NMR sample of the protein in which the target protein is highly deuterated and where NMR visible, isotopic labels have been introduced along the backbone and selectively at ILV side chains as described by Tugarinov and Kay.¹¹ Standard, through-bond double- and triple-resonance NMR spectra are used to obtain the backbone and ILV side chain resonance assignments of the protein. The ligand is then titrated into the protein in small increments such that the shift in both backbone and side chain resonance positions can be readily followed using 2D heteronuclear correlation spectra. Once binding of the compound to the protein is saturated, ¹³C- and ¹⁵N-edited NOESY-HSQC spectra are recorded to generate a set of intermolecular NOEs between the ligand resonances and ILV methyl groups as well as the backbone amide protons of the protein. A known 3D structure or structures of the protein target (or a homology model) is then used for molecular docking using HADDOCK to obtain the protein–ligand structure based solely on the intermolecular NOE restraints.¹² Given that the isotopic labeling method has been used to obtain assignments for large proteins, it is likely that the proposed scheme can also be used to determine experimentally derived molecular models based on sparse NOE data for large protein–small molecule complexes in an efficient yet reliable manner.^{11,13–15} Here the approach is illustrated using the moderately sized 27 kDa N-terminal domain of the molecular chaperone heat shock protein 90 (Hsp90), a known cancer target.

The N-terminal domain of Hsp90 (9–233) was isotopically labeled in *Escherichia coli* according to the published procedure.¹¹ Heteronuclear correlation experiments yielded highly resolved spectra with excellent sensitivity in which all expected methyl peaks can be observed (Figure 1). The triazine **1** had been discovered as a ligand of Hsp90 in a target immobilized NMR screen (TINS) of a fragment library constructed from commercially available compounds.^{16,17} The binding of **1** to Hsp90 was confirmed using surface plasmon

resonance technology, and the equilibrium K_D was determined to be 58 μ M via fitting to a 1:1 binding model (data not shown). We investigated the effect of **1** binding to the protein by recording a high-resolution CT-^[1H,13C] HSQC spectrum in the presence and absence of the compound (Figure 1).^{18,19} The methyl chemical shift perturbations are clear evidence of the binding of **1** to Hsp90. The peak pattern in the bound state is suggestive of a folded protein, indicating that the binding is specific and does not result in protein denaturation or other undesirable effects. Surprisingly, the majority of the methyl resonances are affected by the binding of **1** and a similar pattern was observed in the ^[1H,15N]-HSQC (not shown). Using the sequential assignment determined below, the methyl and backbone amide chemical shift perturbations (CSPs) have been mapped onto the crystal structure of Hsp90 (SI Figure S2). Although the CSPs surround the known ATP binding site, residues far from the site are also significantly affected. The widespread changes in the spectrum of Hsp90 could be indicative of conformational changes in the protein induced or stabilized by the binding of compound **1**. Indeed, conformational changes have been observed for a number of ligands binding to Hsp90.²⁰ Thus it can be difficult to determine the ligand binding site simply on the basis of CSPs (see below). Furthermore, the orientation of the ligand within the binding site, and therefore the nature of the protein–ligand interactions, is not defined by the CSP information.

The sequential backbone assignment of Hsp90 is available (e.g., BMRB 5355) but was confirmed by analysis of TROSY-based HNCACB and HNcoCACB NMR spectra. In total, 76% of the HN, N, $C\alpha$, and $C\beta$ chemical shifts were sequentially assigned, including 87% of the ILV residues. The methyl resonances were subsequently correlated with the intraresidue $C\alpha$ and $C\beta$ assignments by a CCH-TOCSY experiment. Of the ILV residues that had been sequentially assigned, 92% of the ILV methyl assignments were obtained in a straightforward manner. It is not essential to obtain all ILV methyl assignments because only those within the binding site will give rise to intermolecular NOEs. On the basis of the crystal structure of a complex of **1** with Hsp90 (see below), all methyl groups that are within NOE distance (8 Å using a highly deuterated protein) to the ligand have been assigned using only data from these three experiments. Stereospecific methyl assignments for Leu and Val residues were obtained by producing a 10% ¹³C labeled sample and CT-HSQC analysis as described previously.²¹

3D ¹³C-edited and ¹⁵N-edited NOESY-HSQC spectra were recorded on the protein–ligand complex in order to detect intermolecular NOEs.^{22,23} Because of the selective labeling scheme employed, there was minimal overlap among the protein resonances and therefore intermolecular NOEs were unambiguously assigned. Selected strips from the ¹³C-edited NOESY-HSQC and ¹⁵N-edited NOESY-HSQC spectra exhibiting intermolecular NOEs from the ligand are shown in Figure 2A. A total of 21 intermolecular NOEs was identified between resonances of **1** and protein residues, including three to amide protons (I96, G97, and M98) and 18 NOEs to methyl groups (L107, L103, V150, V186, and I96). The peak intensities from the intermolecular NOEs were converted to distances and used as restraints to carry out the docking of the ligand using HADDOCK (see SI for more information).¹²

Typical of many pharmaceutical targets, a crystal structure of apo-Hsp90 (PDB 1YER) is available in the PDB. This structure was the starting point for the experimentally restrained docking

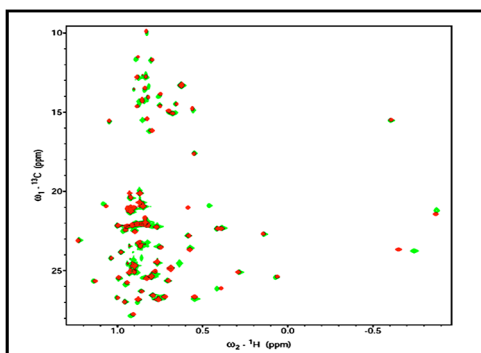


Figure 1. CT- ^[1H,13C] HSQC spectra of an ILV methyl protonated sample of deuterated N-terminal domain of Hsp90 recorded in the absence (in red) and in the presence of **1** (in green) at a protein to ligand ratio of 1:6. Significant chemical shift perturbations for various methyl groups are seen clearly in the presence of **1**, indicative of binding.

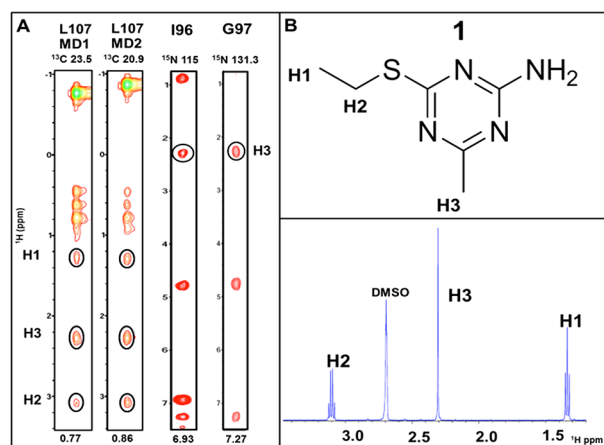


Figure 2. (A) Representative strips from the 3D ^{13}C - and ^{15}N -edited NOESY-HSQC spectra of methyl protonated $\{1(\delta_1 \text{ only}), L-(^{13}\text{CH}_3, ^{12}\text{CD}_3), V(^{13}\text{CH}_3, ^{12}\text{CD}_3)\}$ U- $[^{15}\text{N}, ^{13}\text{C}, ^2\text{H}]$ Hsp90 in the presence of **1**. The intermolecular NOEs between the methyl groups of the protein (L107MD1, L107MD2) and the ligand H1, H2, and H3 groups are circled. The strips for residues I96 and G97 from a ^{15}N -edited NOESY-HSQC spectrum are shown from which intermolecular NOEs to the H3 group of **1** are circled. The frequencies (ppm) of ^1H and ^{13}C or ^{15}N nuclei are shown at the bottom and the top of the strips respectively. (B) The structure (top) and 1D ^1H spectrum (bottom) of **1** in D_2O with the resonance assignment.

procedure. We performed HADDOCK calculations using only the apo-Hsp90 structure and the 21 intermolecular-NOE distances as unambiguous restraints (SI Table S1).¹² The lowest energy cluster exhibited a HADDOCK score and minimal restraint violation energy of -7.0 and 3.8 kcal/mol, respectively, whereas the next ligand cluster exhibited a HADDOCK score of 3.4 and minimal restraint violation energy of 20.0 kcal/mol. The difference between the clusters indicates that the input data defines a single set of structures.

A crystal structure of the complex of **1** with Hsp90 was available in the PDB (3B24).²⁴ In 3B24 there are two protein molecules in the asymmetric unit, and although **1** is bound in the same site in each, it is rotated by approximately 180° in the different structures (Figure 3A). Superposition of the protein in

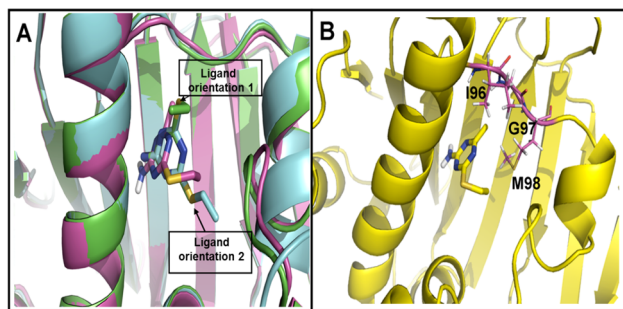


Figure 3. (A) Overlay of the lowest energy HADDOCK model of **1** bound to Hsp90 with a crystal structure of the complex (PDB 3B24) in which **1** binds in two orientations (docked model, magenta; 3B24, green and sky-blue). The orientation of **1** in the NOE-based model is similar to one of the binding modes (seen in sky-blue color) of the ligand in PDB entry 3B24. (B) The orientation of **1** in the docked model is largely determined by the three intermolecular NOEs observed between the H3 group of the ligand and HN of I96, G97, and M98 shown in pink within the protein. The figure was created in PyMOL.²⁷

the three structures (NMR model and two crystal structures) indicates that the sparse NOE method defines the binding site of the ligand uniquely and accurately. Most Hsp90 ligands form critical hydrogen bonds to residues D93 and T184, and these are present in both the X-ray structures and the NMR model. The orientation of **1** in the NMR-based model is quite similar to one of the orientations in the asymmetric unit of the crystal structure (1.7 \AA rmsd). In the NMR model, the orientation of **1** is defined by a network of three intermolecular NOEs from the ligand H3 group to the amide protons of residues I96, G97, and M98 (Figure 3B) and is thus unambiguous. Interestingly, PDB entries 2WI2 and 2WI3 are structures of a similar triazine bound to Hsp90 in which two orientations differing by a 180° axial rotation are found. In this case, the different orientation was dependent on whether soaking or cocrystallization was used to form the complex.²⁵ Taken together the crystal structures suggest that there are two or more low energy conformations for the complex of these simple triazines with Hsp90. In contrast, the NMR data indicate that in solution, there is one predominant conformation and this is likely to be the most physiologically relevant. Importantly, despite the moderate number of intermolecular restraints, the NMR model defines precisely the same binding site as the crystal structure and the critical intermolecular hydrogen bonds, suggesting that in addition to being fast, the method is robust.

Numerous groups have attempted to use CSPs to determine the structure of protein–ligand complexes.^{7,26} We used the ability of HADDOCK to include CSPs as ambiguous restraints for docking and modeled the structure of the Hsp90–**1** complex using the most significant methyl and backbone amide CSPs (SI Figure S3). The HADDOCK calculations generated two clusters whose HADDOCK scores were similar and significantly lower than others. Interestingly, the clusters are both located at the binding site of **1** defined in both the NOE model and the crystal structures. However, despite the fact that electrostatics were used during the HADDOCK calculation, the hydrogen bonds to D93 and T184 are not present. In fact, the amine group of **1** is pointing away from these residues.

Frequently ligand binding is accompanied by a conformational change in the protein. Conformational rearrangement of residues 100–124, which are in close proximity to the ligand binding site of Hsp90, has been observed for a number of ligands including in the two structures in the unit cell of 3B24 (Figure 3A). To investigate any possible influence of conformational rearrangement on the structures calculated from NMR data, we selected three different Hsp90 structures which differ in the conformation of residues 100–124 for docking using HADDOCK.¹² The binding site and orientation of the ligand cluster in each of the three different Hsp90 structures was very similar to that determined using the apoprotein (SI Figure S4). Importantly, the intermolecular hydrogen bonds to D93 and T184 are conserved in all four experimentally constrained docking structures. This data suggests that, at least for the case of Hsp90, binding induced conformational changes do not preclude determining the essential features of a small molecule–protein complex even if those changes are unknown.

CONCLUSION

The method presented here appears to be capable of generating reliable protein–ligand structures in a quick and efficient manner. We have shown that a universal selective labeling scheme can be used to rapidly identify sufficient numbers of

restraints for a small-molecule ligand weakly bound to protein. Moreover, universal labeling precludes the necessity for a priori knowledge of the ligand binding site. However, the present method depends on the availability of selectively labeled, deuterated protein which can only be produced in *E. coli*. Note that the three NOEs involving backbone amide protons of the protein were critical for orienting **1** in the protein–ligand complex. This observation suggests that, at least in some cases, the use of exclusively methyl labeled protein could result in the loss of important constraints for the calculation procedure. Another obvious limitation is the requirement for methyl groups at the ligand binding site. Although ILV residues tend to be well located in proteins and clearly Hsp90 is a good example of this, it is not always the case.¹³ However, it is also possible to selectively label all methyl containing residues, providing even more complete coverage of protein structures and ligand binding sites.²⁸ While we have used standard, through-bond NMR techniques for resonance assignment here, recently steps toward automating the assignment of methyl resonances based either on intramolecular NOEs and/or through-space paramagnetic effects have been taken.²⁹ Implementation of selective methyl labeling in conjunction with automated resonance assignment should enable structure determination of complexes involving reasonably large proteins up to 75 kDa. We feel the present method could prove valuable for the early stages of FBDD by providing 3D structure information on weakly binding fragment–protein complexes.

■ ASSOCIATED CONTENT

Supporting Information

Detailed description of sample preparation and NMR methods and figures. This material is available free of charge via the Internet at <http://pubs.acs.org>.

■ AUTHOR INFORMATION

Corresponding Author

*Phone: +31-71527-4543. E-mail: g.siegal@chem.leidenuniv.nl.

Present Address

¹ZoBio BV, Leiden 2300RA, The Netherlands.

Notes

The authors declare the following competing financial interest(s): GS acknowledges greater than 5% ownership of ZoBio, a company that provides research services in drug discovery.

■ ACKNOWLEDGMENTS

We thank Dr. Hans Wienk for his assistance and the SONNMRLSF in Utrecht. We also acknowledge the contribution to Hsp90 crystallography from Thomas A. Ceska at UCB, UK.

■ REFERENCES

- (1) Volarath, P.; Harrison, R. W.; Weber, I. T. Structure based drug design for HIV protease: from molecular modeling to cheminformatics. *Curr. Top. Med. Chem.* **2007**, *7* (10), 1030–1038.
- (2) Hardy, L. W.; Malikayil, A. The impact of structure-guided drug design on clinical agents. *Curr. Drug Discovery* **2003**, *3*, 15–20.
- (3) Hajduk, P. J.; Greer, J. A decade of fragment-based drug design: strategic advances and lessons learned. *Nature Rev. Drug Discovery* **2007**, *6*, 211–219.
- (4) Oltersdorf, T.; Elmore, S. W.; Shoemaker, A. R.; Armstrong, R. C.; Augeri, D. J.; Belli, B. A.; Bruncko, M.; Deckwerth, T. L.; Dinges, J.; Hajduk, P. J.; Joseph, M. K.; Kitada, S.; Korsmeyer, S. J.; Kunzer, A.

R.; Letai, A.; Li, C.; Mitten, M. J.; Nettesheim, D. G.; Ng, S.; Nimmer, P. M.; O'Connor, J. M.; Oleksijew, A.; Petros, A. M.; Reed, J. C.; Shen, W.; Tahir, S. K.; Thompson, C. B.; Tomaselli, K. J.; Wang, B.; Wendt, M. D.; Zhang, H.; Fesik, S. W.; Rosenberg, S. H. An inhibitor of Bcl-2 family proteins induces regression of solid tumours. *Nature* **2005**, *435*, 677–681.

(5) Shuker, S. B.; Hajduk, P. J.; Meadows, R. P.; Fesik, S. W. Discovering high-affinity ligands for proteins: SAR by NMR. *Science* **1996**, *274*, 1531–1534.

(6) Krishnamoorthy, J.; Yu, V. C. K.; Mok, Y.-K. Auto-FACE: an NMR based binding site mapping program for fast chemical exchange protein–ligand systems. *PLoS One* **2010**, *5* (2), e8943.

(7) Schieborr, U.; Vogther, M.; Elshorst, B.; Betz, M.; Grimme, S.; Pescatore, B.; Langer, T.; Saxena, K.; Schwalbe, H. How much NMR data is required to determine a protein–ligand complex structure? *ChemBioChem* **2005**, *6* (10), 1891–1898.

(8) Pellecchia, M.; Meininger, D.; Dong, Q.; Chang, E.; Jack, R.; Sem, D. S. NMR-based structural characterization of large protein–ligand interactions. *J. Biomol. NMR* **2002**, *22*, 165–173.

(9) Constantine, K. L.; Davis, M. E.; Metzler, W.; Mueller, L.; Claus, B. L. Protein–ligand NOE matching: a high-throughput method for binding pose evaluation that does not require protein NMR resonance assignments. *J. Am. Chem. Soc.* **2006**, *128*, 7252–7263.

(10) Yu, L.; Sun, C.; Song, D.; Shen, J.; Xu, N.; Gunasekera, A.; Hajduk, P. J.; Olejniczak, E. T. Nuclear magnetic resonance structural studies of a potassium channel–charybdotoxin complex. *Biochemistry* **2005**, *44*, 15834–15841.

(11) Tugarinov, V.; Kay, L. E. Ile, Leu, and Val methyl assignments of the 723-residue malate synthase G using a new labeling strategy and novel NMR methods. *J. Am. Chem. Soc.* **2003**, *125*, 13868–13878.

(12) De Vries, S. J.; Van Dijk, M.; Bonvin, A. M. J. J. The HADDOCK web server for data-driven biomolecular docking. *Nature Protoc.* **2010**, *5*, 883–897.

(13) Sprangers, R.; Kay, L. E. Quantitative dynamics and binding studies of the 20S proteasome by NMR. *Nature* **2007**, *445*, 618–622.

(14) Sibille, N.; Hanouille, X.; Bonachera, F.; Verdegem, D.; Landrieu, I.; Wieruszkeski, J. M.; Lippens, G. Selective backbone labelling of ILV methyl labelled proteins. *J. Biol. Mol.* **2009**, *43* (4), 219–227.

(15) Tugarinov, V.; Choy, W. Y.; Orekhov, V. Y.; Kay, L. E. Solution NMR-derived global fold of a monomeric 82 kDa enzyme. *Proc. Natl. Acad. Sci. U. S. A.* **2005**, *102*, 622–627.

(16) Vanwetswinkel, S.; Heetebrij, R. J.; Van Duynhoven, J.; Hollander, J. G.; Filippov, D. V.; Hajduk, P. J.; Siegal, G. TINS, target immobilized NMR screening: an efficient and sensitive method for ligand discovery. *Chem. Biol.* **2005**, *12*, 207–216.

(17) Siegal, G.; AB, E.; Schultz, J. Integration of fragment screening and library design. *Drug Discovery Today* **2007**, *12*, 1032–1039.

(18) Palmer, A. G., III; Cavanagh, J.; Wright, P. E.; Rance, M. Sensitivity improvement correlation NMR spectroscopy. *J. Magn. Reson.* **1991**, *93*, 151–170.

(19) Schleucher, J.; Schwendinger, M.; Sattler, M.; Schmidt, P.; Schedletsky, O.; Glaser, S. J.; Sorensen, O. W.; Griesinger, C. A general enhancement scheme in heteronuclear multidimensional NMR employing pulsed field gradients. *J. Biomol. NMR* **1994**, *4*, 301–306.

(20) Murray, C. W.; Carr, M. G.; Callaghan, O.; Chessari, G.; Congreve, M.; Cowan, S.; Coyle, J. E.; Downham, R.; Figueroa, E.; Frederickson, M.; Graham, B.; McMenamin, R.; O'Brien, A. M.; Patel, S.; Phillips, T. R.; Williams, G.; Woodhead, A. J.; Woolford, A. J.-A. Fragment-based drug discovery applied to Hsp90. Discovery of two lead series with high ligand efficiency. *J. Med. Chem.* **2010**, *53* (16), 5942–5955.

(21) Neri, D.; Szyperski, T.; Otting, G.; Senn, H.; Wuthrich, K. Stereospecific nuclear magnetic resonance assignments of the methyl groups of valine and leucine in the DNA-binding domain of the 434 repressor by biosynthetically directed fractional ¹³C labeling. *Biochemistry* **1989**, *28*, 7510–7516.

(22) Kay, L. E.; Keifer, P.; Saarinen, T. Pure absorption gradient enhanced heteronuclear single quantum correlation spectroscopy with improved sensitivity. *J. Am. Chem. Soc.* **1992**, *114*, 10663–10665.

(23) Davis, A. L.; Keeler, J.; Laue, E. D.; Moskau, D. Experiments for recording pureabsorption heteronuclear correlation spectra using pulsed field gradients. *J. Magn. Reson.* **1992**, *98*, 207–216.

(24) Miura, T.; Fukami, T.; Hasegawa, K.; Ono, N.; Suda, A.; Shindo, H.; Yoon, D. O.; Kim, S. J.; Na, Y. J.; Aoki, Y.; Shimma, N.; Tsukuda, T.; Shiratori, Y. Lead generation of heat shock protein 90 inhibitors by a combination of fragment-based approach, virtual screening, and structure-based drug design. *Bioorg. Med. Chem. Lett.* **2011**, *21*, 5778–5783.

(25) Brough, P. A.; Barril, X.; Borgognoni, J.; Chene, P.; Nicholas, G. M.; Davies, Davis, B.; Drysdale, M. J.; Dymock, B.; Eccles, S. A.; Garcia-Echeverria, C.; Fromont, C.; Hayes, A.; Hubbard, R. E.; Jordan, A. M.; Jensen, R. M.; Massey, A.; Merrett, A.; Padfield, A.; Parsons, R.; Radimerski, T.; Raynaud, F.; Robertson, A.; Roughley, S.; Schoepfer, R.; Simmonite, H.; Sharp, S.; Surgenor, A.; Valenti, M.; Walls, S.; Webb, P.; Wood, M.; Workman, P.; Wright, L. Combining hit identification strategies: fragment-based and in silico approaches to orally active 2-aminothieno[2,3-*d*]pyrimidine inhibitors of the Hsp90 molecular chaperone. *J. Med. Chem.* **2009**, *52* (15), 4794–4809.

(26) Stark, J.; Powers, R. Rapid protein–ligand costructures using chemical shift perturbations. *J. Am. Chem. Soc.* **2008**, *130*, 535–545.

(27) *The PyMOL Molecular Graphics System*, version 1.2r3pre; Schrödinger, LLC: Portland, OR.

(28) Otten, R.; Chu, B.; Krewulak, K. D.; Vogel, H. J.; Mulder, F. A. A comprehensive and cost-effective NMR spectroscopy of methyl groups in large proteins. *J. Am. Chem. Soc.* **2010**, *132* (9), 2952–2960.

(29) Venditti, V.; Fawzi, N. L.; Clore, G. M. Automated sequence- and stereospecific assignment of methyl-labeled proteins by paramagnetic relaxation and methyl–methyl nuclear Overhauser enhancement spectroscopy. *J. Biomol. NMR* **2011**, *51*, 319–328.